Journal of Molecular Graphics and Modelling 44 (2013) 33–43

Contents lists available at ScienceDirect

Journal of Molecular Graphics and Modelling

journal homepage: www.elsevier.com/locate/JMGM

Molecular dynamics simulation of single-walled silicon carbide nanotubes immersed in water

Fariba Taghavi [a], Soheila Javadian [a,*], Seyed Majid Hashemianzadeh [b,*]

[a] Department of Physical Chemistry, Tarbiat Modares University, P.O. Box 14115-117, Tehran, Iran
[b] Molecular Simulation Research Laboratory, Department of Chemistry, Iran University of Science and Technology, Tehran, Iran

ARTICLE INFO

Article history:
Accepted 27 April 2013
Available online 14 May 2013

Keywords:
Molecular dynamics simulation
Single-walled silicon carbide nanotube (SWSiCNT)
Confined water
Radial density profile
Diffusion coefficient (D)

ABSTRACT

The structure and dynamics of water confined in single-walled silicon carbon nanotubes (SWSiCNTs) are investigated using molecular dynamics (MD) simulations. The density of water inside SWSiCNTs is reported, and an equation is suggested to predict the density of water inside SWSiCNTs. Interestingly, the water diffusion coefficients (*D*) here are larger compared with those in SWCNTs and single-walled boron-nitride nanotubes (SWBNNTs). Furthermore, water inside zigzag SWCNTs has a lower diffusion coefficient than water inside armchair SWCNTs. A thorough analysis of the density profiles, hydrogen bonding, and water molecule orientation inside SWSiCNTs is presented to explore the mechanism behind the diffusive behavior of water observed here. It is shown here, by mean square displacement (MSD) analysis, that water molecules inside SWSiCNTs diffuse with a ballistic motion mechanism for up to 500 ps. Additionally it is confirmed here for the first time that water molecules confined in the SWSiCNTs with diameters of less than 10 Å obey the single-file diffusion mechanism at time scales in excess of 500 ps. The orientation of water molecules inside SWSiCNTs could be a good explanation for the difference between the diffusion coefficient in (6,6) and (10,0) SWSiCNTs. Finally, a PMF analysis explains the difficulty of water entrance into SWSiCNTs and also the different water self-diffusion inside armchair and zigzag SWSiCNTs. These results are motivating reasons to use SWSiCNTs in nanoscale biochannels, for instance, in drug-delivery applications.

1. Introduction

The use of water in nanoscale confinement is of growing interest in nanofluidic devices [1,2], biomimetic nanoscale devices [3], and nanoelectronics [4]. In addition, the unique structure and dimensions of nanotubes have motivated the use of water-filled. Single-walled silicon carbide nanotube (SWCNTs) as an ideal model for understanding the primary behavior of confined nanofluid systems. It is assumed that the static and dynamic behaviors of water in and outside of a nanoscopic pore are absolutely different from those of the bulk liquid due to nanoscale confinement effects [5,6].

In recent years, the behavior of water molecules in SWCNTs has been comprehensively studied using experiments [7–9] and computations [10–13]. The main result of investigations into the microscopic static structure of water inside SWCNTs has been the identification of an alteration in the hydrogen bonding network of water in nanoscale confinement. For example, in 2004, Wang et al. estimated the best diameter of an SWCNT that can hold layers of water molecules [14]. In 2005, Alexiadis et al. recognized three principle structures of confined water inside SWCNTs due to their sizes. In nanotubes with diameters less than 9 Å, water adopts a single-file or wire structure due to the confinement effects. In larger nanotubes, a layered structure is the dominant structure for water, but in SWCNTs with diameters larger than 25 Å, the static and dynamic behaviors of water are similar to those of the bulk [11]. In another work, they proposed a correlation between the density of water inside SWCNTs and the nanotube diameter [15]. In contrast, owing to the difficulties involved in performing reliable experimental studies on the transport properties, i.e., the self-diffusion coefficient of nanoconfined fluids, many characteristics of the dynamical behavior of these systems are not yet clearly understood. Recently, molecular dynamics (MD) simulations have begun to play an important role in the development of theories of transport in confined water inside SWCNTs. Martí and Gordillo estimated that the diffusivity of water inside SWCNTs in the tube axis direction is faster than that of bulk water [16]. However, Marañón Di Leo and Marañón proved that confined water in SWCNTs has a lower diffusivity than bulk water [17]. Allen et al. reported a comprehensive study of the structure and diffusion of water confined inside microscopic channels [18]. They showed that the axial self-diffusion coefficient of water in hydrophobic channels

* Corresponding authors. Fax: +98 21 82883455.
E-mail addresses: javadian_s@modares.ac.ir, javadians@yahoo.com (S. Javadian), hashemianzadeh@yahoo.com (S.M. Hashemianzadeh).

1093-3263/$ – see front matter © 2013 Elsevier Inc. All rights reserved.
http://dx.doi.org/10.1016/j.jmgm.2013.04.012

is lower than that of bulk water but that it does not demonstrate a monotonic diameter dependence because the noticeable decrease in the diffusion coefficient is associated with the hydrogen bonding network of water molecules. Mashl et al. reported results in agreement with those of Allen et al. They also established that the axial diffusion coefficient of water inside (9,9) CNTs was significantly lower compared with that inside CNTs with different diameters, although the general tendency was that the diffusion coefficient decreased with decreasing diameter [19]. In another study, the effect of quantum partial charges on the structure and dynamics of water in single-walled carbon nanotubes was investigated, and the water diffusion coefficient was found to increase in the presence of the partial charges [20]. The diffusion mechanism of water clusters within infinitely long, narrow SWNTs was investigated in several studies [13,21,22]. For example, Striolo et al. reported that a Fickian-type diffusion mechanism prevails over other mechanisms, such as single-file or ballistic diffusion for water molecules, inside narrow SWCNTs for up to 500 ps time scales [13].

More recently, while working with SWCNTs, especially in biosystems [23], there have been widespread reports on the successful synthesis of SWBNNTS and SWSiCNT as new nanotube systems [24–27]. SWBNNTs have been found to have interesting applications in biological nanofluidic systems [28]. Won and Aluru reported that the wetting behavior of water inside a subnanometer BNNT is better than that of a CNT with a similar diameter. They also observed that the wetting behavior of a (5,5) SWBNNT improved in the presence of partial charges [29].

The stability, electronic structure, and properties of SWSiCNTs have been studied using theoretical approaches [30–35]. For instance, Mavrandonakis et al. established that SWSiCNTs with a Si-to-C ratio of 50:50 are energetically more stable than the forms that contain C—C or Si—Si bonds [35]. After that, Alam et al. showed that an arrangement of SWSiCNT that contains alternating Si and C atoms, with each Si atom having three C neighbors and vice versa, is the most stable one [36,37]. In addition, it has been established that SWSiCNTs have a high thermal stability and a wide bandgap, that they can be simply doped, and that the purity concentration of defects is easily manageable [34,38,39]. Consequently, because SWSiCNTs have unique characteristics compared with carbon-based nanotubes (SWCNTs), it would be interesting to analyze the static and dynamic behavior of water confined inside these types of nanotubes as a simple model of a nanoscale biochannel for transporting water or ions or as a nanoscale molecular device. Khademi and Sahimi performed a molecular dynamics simulation of pressure-driven water flow in some zigzag silicon-carbide nanotubes. They reported that all the SWSiCNTs that were examined produced higher flow enhancements than CNTs and required smaller pressure gradients to do so [40].

To the best of our knowledge, very few studies have been performed on the structures and dynamics of water molecules confined inside armchair and zigzag SWSiCNTs [40–42], and none of them contain a systematic analysis of the confinement effects on the density, distribution, and diffusion of water molecules confined inside armchair and zigzag SWSiCNTs. Yang et al. [41] chose the number of water molecules inside the SWSiCNT to give a number density comparable to that of bulk water.

In this work, we carried out MD simulations to clarify, at the molecular level, the static and dynamic behavior of water molecules confined in SWSiCNTs and to investigate the helicity and nanotube diameter effects on these properties. In the following sections, the simulation methods and model, density, MSD, diffusion coefficients, radial density profiles, hydrogen bonding network among water molecules confined inside SWSiCNTs and orientation of water molecule dipole moments are explained. Finally, in the conclusion section, interesting outcomes of our simulation studies are clarified.

Table 1
The Lennard–Jones parameters (ε and σ) and partial charges (q) for water and SWSiCNT atoms.

Site	ε (kJ mol^{-1})	σ (Å)	q (e)
O	0.6364	3.1506	−0.834
C	0.3598	3.4	0.45
Si	1.9619	3.7364	−0.45

2. Models and simulation methods

All MD simulations were performed in an NPT ensemble at 300 K and 1 atm with a Berendsen thermal bath and a Berendsen barostat [43] (expect for the diffusion calculations, which were performed in an NVT ensemble with a temperature of 300 K) using the DL_POLY Classic software package [44]. The structural properties of each SWSiCNT in this study were taken from Refs. [36,37], and the SWSiCNTs in the MD simulations were considered to be fixed with respect to the center of the simulation box. Water molecules were described by the TIP3P model [45]. Short-range interaction potentials were represented by a Lennard–Jones potential [46] using the Lorentz–Berthelot combining rule [47], while long-range coulombic interactions were handled by the Ewald sum (which is reliable because it properly reproduces the adsorption capacity of the SWSiCNTs) [46]. Table 1 summarizes all the Lennard–Jones parameters and partial charge values (provided from density functional theory calculations) [35] used in the MD simulations. The nonbonded cutoff was 13 Å, and the quadrupole interactions were not considered in our simulations because they have a minuscule effect on the resultant water structure [48].

The leap-frog Verlet integration algorithm [47] with a time step of 1 fs was considered for integration of the equations of motion. The MD simulations were initially performed in an equilibration stage of 1 ns, and then simulation trajectories were saved every 200 fs in each production run of 3 ns, expect for diffusion calculations, which have much larger production times of 1 μs. The structural analyses for two sets of data of 3 ns and 1 μs does not show notable differences therefore, the 3 ns production time will be reported for structural analyses in the following sections. All simulation cells contain a finite nanotube in a box of bulk water with 3D periodic boundary conditions. The simulated systems are listed in Table ST2 in the supporting material, including the diameter of the SWSiCNTs (d), the number of carbon and silicon atoms in each nanotube (N_C and N_{Si} are equal to keep the nanotube natural), the number of water molecules in the simulation box (N_W), the length of the nanotube (l) and size of the simulation box ($a \times b \times c$) for each case. To evaluate the reliability of the calculated equilibration, the tendency of the properties of interest (especially the potential and total energy) as a function of the simulation time were studied, and it was observed that there was no evidence of a sharp deviation in the tendencies of these properties (Supporting information SF1).

Before introducing the simulation outcomes, it is necessary to explain how to prepare the initial configurations. To examine how the density of water inside the nanotube in the initial configuration affects the simulation results, two main initial configurations were prepared. One initial configuration contained water molecules with a density equal to the bulk density all over the simulation box, even inside the SWSiCNT. In the other initial configuration, the nanotube was considered to be empty, and the water molecules were randomly distributed outside of the nanotube with the density of bulk water. The simulation results showed that the final overall density inside the SWSiCNT would be the same in both cases despite the different initial densities, but the time to reach equilibration was noticeably longer with the empty SWSiCNT. Supporting information FS2 shows that the narrowest nanotubes remain dry at thermodynamic equilibrium and water density within the wider

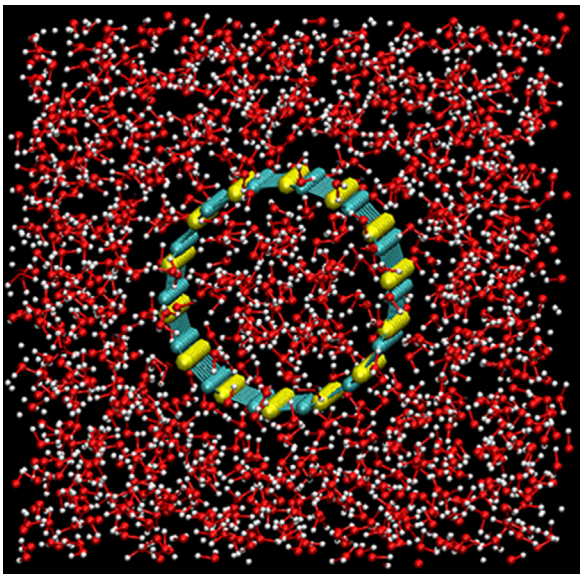

Fig. 1. The initial configuration of a (7,0) SWSiCNT in its simulation box contains water molecules distributed randomly with the density of the bulk.

nanotube is the same irrespective of whether they start filled or empty of water. Therefore, the first case of water-filled nanotube was chosen for all subsequent simulations to optimize the simulation time. In Fig. 1, the initial configuration of (7,7) SWSiCNT in its simulation box is illustrated.

3. Results and discussion

3.1. Overall density of confied water

The equilibrium number of water molecules inside SWSiCNTs could be clearly delimited even though the water molecules repeatedly enter and leave the nanotubes. For SWCNTs, there are few studies [15,49,50] describing the expected density of water molecules when considering the entrance of water molecules from an outer bath, and there are no reports about the natural density of water inside SWSiCNTs. Alexiadis et al. [15] suggested an equation for developing a correlation between the CNT diameter and the water density. His results, which represent a good approximation for all the water model/CNT rigidity combinations, are provided in Fig. 2 for comparison with our results.

Here, the first results showing the influence of confinement and nanotube helicity on the number of water molecules inside the SWSiCNTs are presented. In SWSiCNTs with diameters d ranging between 8.6 Å and 24.8 Å, water molecules form layered structures

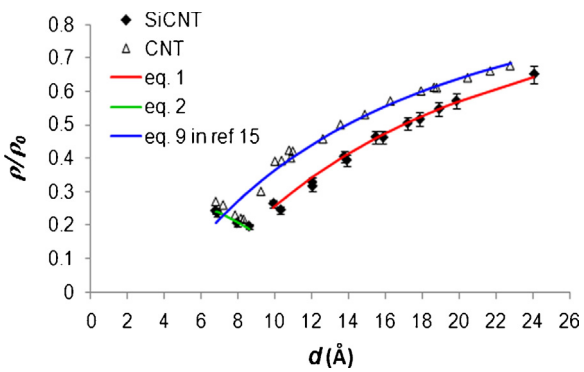

Fig. 2. Overall water density inside SWCNTs from Ref. [15] and inside SWSiCNTs in comparison with data suggested from Eqs. (2) and (3).

inside SWSiCNTs, as will be discussing in the next section. The correlation between the time-averaged overall water density ρ inside nanotubes and nanotube diameters could be presented as follows (see Fig. 2):

$$\frac{\rho}{\rho_0} = 1 - \frac{\rho^*}{\left((d/d*)+1\right)^2} \quad \text{for} \quad d > 8.6 \ \text{Å} \tag{1}$$

$$d^* = 21.5 \ \text{Å}, \quad \rho^* = 1.6 \ \text{g/cm}^3$$

where d is the nanotube diameter and ρ_0 is the bulk water density. This equation is a modification of what has been reported before [15] for SWCNTs.

In contrast, in narrower SWSiCNTs, the overall density of water inside the nanotubes decreases as the tube diameter increases, as shown in Fig. 2. In these narrow nanotubes, surface effects (driven approximately 2.8 Å in the preceding section) are not negligible compared with the tube diameter ($d < 8.6$ Å). Apparently, the confinement effects are considerable inside narrow SWSiCNTs, and confined water molecules do not behave like bulk water inside. Therefore, a correction coefficient considering the repulsion distances of carbon and silicon atoms (σ_{SiO} and σ_{CO}), which are responsible for the surface effects here, could be appropriate. The following suggested corrected density could be considered:

$$\rho' = \left(\frac{\rho}{\rho_0}\right) \left(0.053\left(\frac{d-\sigma}{d}\right)^{5.98}\right) \quad \text{for} \quad d < 8.6\,\text{Å} \tag{2}$$

In this equation, σ is defined as $\sigma = (\sigma_{CO} + \sigma_{SiO})/2$, ρ' is the corrected water density inside narrow SWSiCNTs, d is the nanotube diameter, and (ρ/ρ_0) is defined the same way as it was in Eq. (1). The correction factor in this equation evidently confirms that the overall density in the narrower SWSiCNTs is strongly affected by the available diameter of the nanotubes, $(d-\sigma)$. Fig. 2 clearly shows that a combination of Eqs. (1) and (2) would be sufficient for predicting the water density inside SWSiCNTs. It has to be mentioned that in Fig. 2, the uncertainties are not large especially for the narrow SWSiCNTs (about 4%). So, it could be reliable to say that a qualitative change in behavior of the density of confined water inside SWSiCNTs happens in the lower nanotube diameter points.

Note that using two equations to fit the density vs. nanotube diameter data is necessary because in the smaller nanotubes, the value of the repulsion distance parameters of carbon and silicon atoms (σ_{SiO} and σ_{CO}) are considerable in comparison with the nanotube diameter. These parameters are imported into the equation for narrower nanotubes to consider the effective diameter of the nanotube $(d-\sigma)$ instead of the pure diameter d. In addition, if a parabolic-type equation was used for fitting the entire range of nanotube diameter data, it would be impossible to suggest the limit value for nanotube diameter (approximately 150 Å) in which the density of water inside SWSiCNTs is equal to the bulk value of the density. As well, a quantitative analysis of the second-order Akaike Information Criterion (AIC_c) of the two options of a single parabolic-type equation and two piecewise equations for nanotube diameters larger and smaller than 8.6 Å shows an AIC_c equals to 24.12 for the parabolic function (single equation for all points), 18.86 for Eq. (1) ($d > 8.6$ Å) and 19.81 for Eq. (2) when ($d < 8.6$ Å). Therefore, the use of two piecewise functions is the best candidate model here.

3.2. MSD and self-diffusion coefficients

The transport behavior of water may undergo significant changes from those of the liquid bulk when it is confined in nanoscale geometries. These changes have been detected in some cases of water molecules confined inside SWCNTs and SWNBNTs [13,29]. Understanding the mechanism of confined water diffusion in nanoscale geometries is the objective of this section. Here,

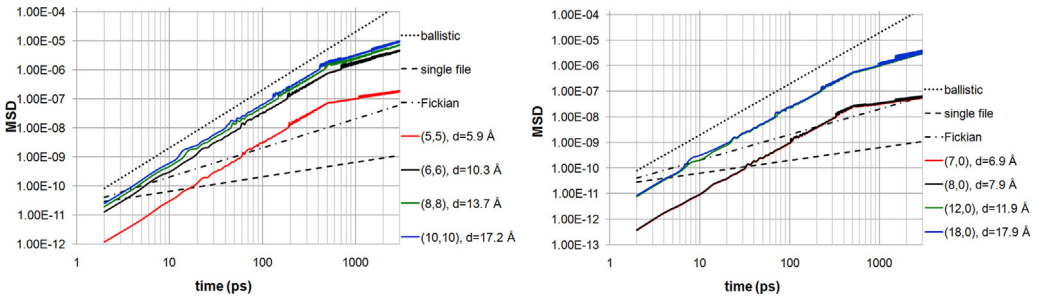

Fig. 3. Mean square displacements in the direction of the nanotube axis, MSD, vs. time (ps) for water molecules confined inside armchair (left) and zigzag (right) SWSiCNTs. The scaling behavior anticipated for diffusion mechanisms of the ballistic (dotted), single-file (dashed), and Fickian (dot-dashed) types are also shown.

the results of calculations of the mean square displacement (MSD) and the self-diffusion coefficient (D) of oxygen atoms in water molecules confined inside armchair and zigzag SWSiCNTs are reported to investigate the mechanism behind the diffusive behavior of water confined in these type of nanotubes. The diffusion coefficients are considered only for oxygen atoms because the center of mass of the water molecule is approximately located on the oxygen atom.

In diffusion studies, the motion of confined water is often considered to obey the Fickian mechanism [51], even in narrow nanotubes [20,52]. It has to be assumed that the Fickian motion only occurs when water molecules are able to pass each other. This assumption is questionable if it is assumed that in narrow SWSiCNTs with a distribution of partial charges on the tube walls, water molecules may not be able to not pass each other easily. The MSD of particles following Fickian diffusion is defined as follows:

$$dz^2 \propto D_z dt \tag{3}$$

In this equation, dz^2 is the MSD in the tube axis direction, D is the diffusion coefficient along the nanotube axis, and dt is time. However, the number of partial charges on the SWSiCNTs (approximately $\pm 0.45e$) encourages investigation of the possibility of other diffusive mechanisms (single-file and ballistic modes) here. Single-file mode diffusion is characterized by a situation in which molecules are unable to pass each other in pores or channels and expressed as [53]:

$$dz^2 \propto Bdt^{1/2} \tag{4}$$

where B is the diffusion mobility.

The last diffusion mechanism, the ballistic, occurs when confined water molecules move in a highly coordinated style and has the following general form:

$$dz^2 \propto Cdt^2 \tag{5}$$

where C is a proportionality coefficient.

The actual mechanism of water diffusion could be understood from the scaling behavior of the MSD as a function of time in Eqs. (4)–(6). Fig. 3 demonstrates the MSD in the direction of the tube axis for water confined inside armchair (left) and zigzag (right) SWSiCNTs. As revealed in this figure, the diffusion mode of all types of SWSiCNTs is ballistic for the first several hundred picoseconds of production time. However, for times longer than 500 ps, the trends of the MSD change, and a difference between narrow and wider SWSiCNTs can be established. In narrower SWSiCNTs, such as (7,0), (8,0), and (5,5), the MSDs are a function of $\sqrt{t}$, suggesting a single-file mechanism for the diffusion coefficient (Fig. 3). This is the first time that the diffusion coefficients of water inside nanotubes are shown to follow single-file mechanisms; the other types of narrow nanotubes, such as SWCNTs and SWBNNTs, have been shown to have a Fickian-type diffusion mechanism [13,29]. The single-file mechanism may be observed in narrow SWSiCNTs because of the effect of partial charges on the walls of nanotubes that make it difficult for water molecules to pass each other. In contrast, in wider SWSiCNTs such as (8,8), (10,10), (16,0), and (18,0), the MSD changes linearly as a function of time, exhibiting a Fickian-type diffusion mechanism. This behavior can be deduced by considering the additional space available for water molecules in wider SWSiCNTs in addition to the collective motion of water molecules due to the hydrogen bonding network between them.

The axial diffusion coefficients for water molecules in SWSiCNTs of various nanotube diameters for the mechanisms that have been reported above are shown in Fig. 4. It has to be mentioned that the diffusion coefficients in this figure are computed by fitting the diffusive or post-ballistic regime in a linear way for Fickian mechanism and with an equation with type of Eq. (5) for Single-file mode. The temporal range of this fitting is over 600 ps for armchair and zigzag SWSiCNTs. The diffusion coefficient of water confined inside the SWSiCNTs is notably less than that in the bulk, 2.68×10^{-9} m^2/s (calculated in this study to estimate the validity of the results) but is larger than that in SWCNTs [54,55] and SWBNNTs [29]. These results show that water molecules confined inside

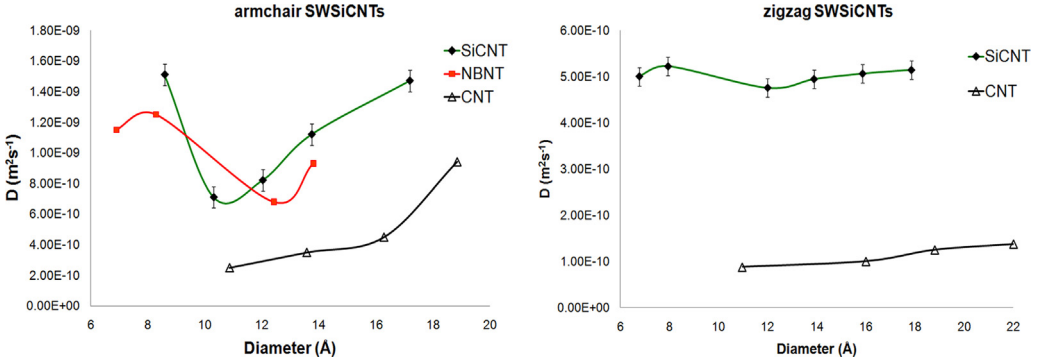

Fig. 4. Averaged axial diffusion coefficient of water inside armchair (left) and zigzag (right) SWCNTs (Refs. [53,54]), SWBNNTs (Ref. [28]), and SWSiCNTs.

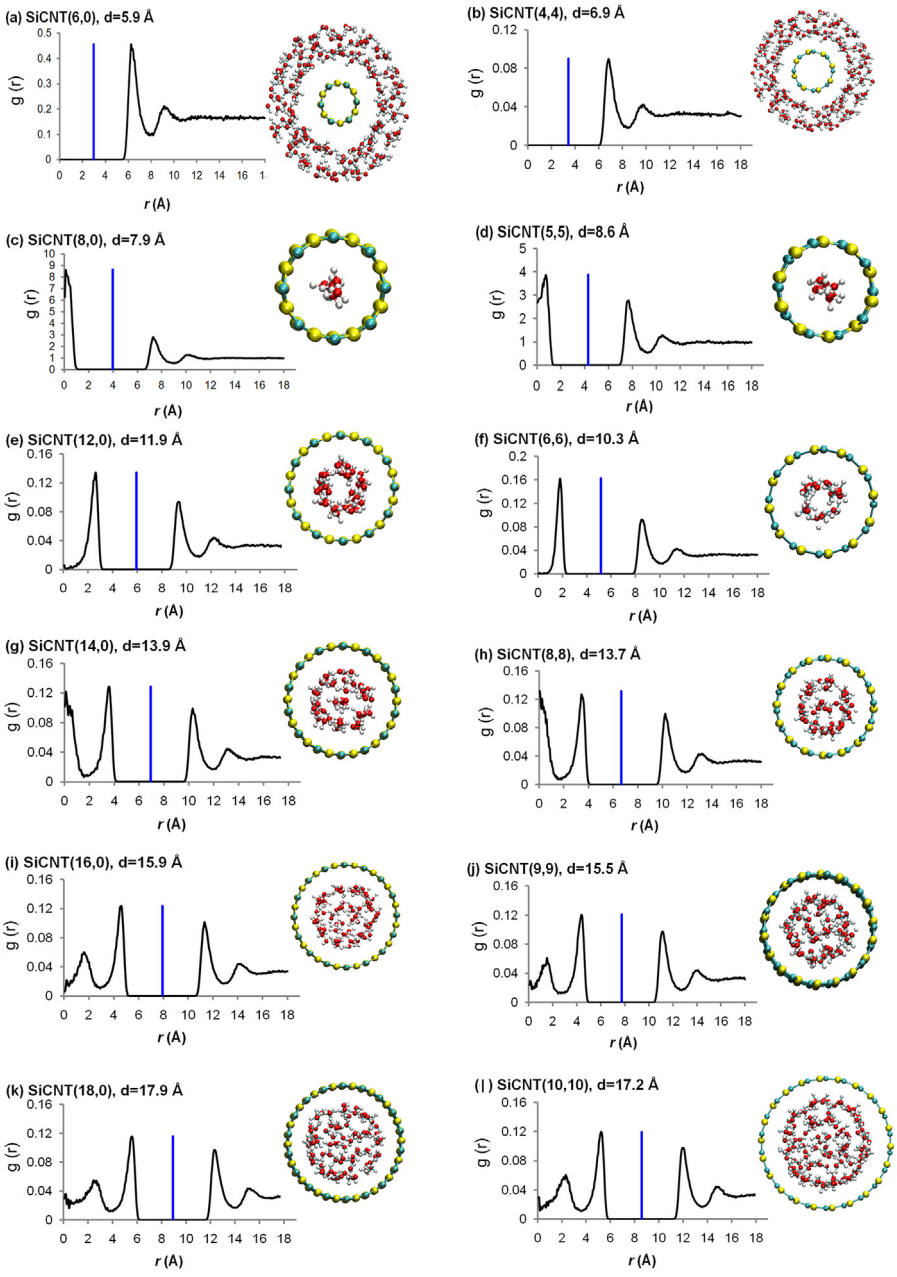

Fig. 5. Radial density profiles of oxygen water molecules confined inside SWSiCNTs. The blue line shows the location of the nanotube wall. Water molecules outside nanotubes are deleted for clear depiction (expect for the empty ones). *Note*: Scales are not considered in this figure. (For interpretation of the references to colour in this figure legend, the reader is referred to the web version of the article.)

SWSiCNTs diffuse faster than when inside SWCNTs and SWBNNTs. These results may be related to the number of partial charges on Si and C atoms that attract water molecules inside the SWSiCNTs faster than inside the other types of nanotubes. These results also suggest that the diffusion of confined water molecules is affected by their configurations inside the SWSiCNTs. In addition, Fig. 4 (right) shows that the diffusion coefficient of water molecules inside narrow SWSiCNTs is increased with increasing nanotube diameters from (7,0) to (8,0). For wider SWSiCNTs, the diffusion coefficient suddenly decreases when moving from (8,0) to (12,0) SWSiCNTs and increases again in (14,0) SWSiCNTs. Furthermore, the diffusive behavior of water molecules inside armchair SWSiCNTs exhibits a similar trend to that shown in Fig. 4 (left), but the diffusion is faster in these nanotubes than in the zigzag ones. The faster diffusion of single-file water structures inside armchair SWSiCNTs vs. the zigzag ones is explained more at the end of Section 3.5. The diffusive behavior of water molecules inside SWSiCNTs is consistent with what has been reported for SWBNNTs previously [29] and could be understood in more detail by investigating the configuration and hydrogen bonding network of the water molecules inside these tubes, which is discussed next.

3.3. Radial density profiles

The configuration of water molecules inside SWCNTs has been an interesting subject in recent years [6,14,19,56–59]. All these studies revealed the nanoscale confinement effects cause a heterogeneous distribution of water molecules in the interior of SWSiCNTs, chiefly in the direction of the main axis of the nanotube as the main direction of confinement [58], in spite of the fact that the conditions and the computational details were quite different in these studies. To determine the diameter or confinement effects

on the configuration of water molecules inside SWSiCNTs and to compare them with previous reports on SWCNTs, the oxygen density profile could be used instead of the density profile of the water molecule because the center of mass of a water molecule is located very close to the oxygen atom. It should be mentioned again that the nanotube and water molecule structures are considered to be fixed and that in smaller-diameter tubes, buckling of the structure occurs, which may affect the results.

Fig. 5 exhibits the time-averaged radial distribution function, $g(r)$, that was calculated in cylindrical layers ($\Delta r = 0.0625$ Å) centered at the axis of the SWSiCNT and plotted as a function of the cylindrical radius r. The commensurate snapshot configuration of water molecules inside SWSiCNTs is shown in Fig. 5 as well. The characteristic tendencies in these profiles are comparable to those of water inside SWCNTs with the same diameters, although the peak positions are shifted to a larger radius (about 1.5 Å) in SWSiCNTs owing to the larger size and stronger repulsion force of silicon atoms [14].

Fig. 5(a) and (b) shows that water molecules could not enter (6,0) and (4,4) SWSiCNTs (with 5.95 Å and 6.87 Å diameters, respectively), while, as revealed in (Fig. 5(c) and (d)), one-dimensional single-file (wire) structures of water molecules were formed in (7,0) (this tube is not shown in Fig. 5), (8,0) and (5,5) nanotubes (with 6.95 Å, 7.94 Å and 8.59 Å diameters, respectively). Therefore, (7,0) and (5,5) SWSiCNTs are the smallest zigzag and armchair SWSiCNTs that contain water molecules inside. The formation of a single-file structure inside (5,5) SWSiCNTs have previously been proven by first-principles calculations [41]. For SWCNTs, (5,5) and (10,0) nanotubes (with diameters of 6.7 Å and 7.8 Å, respectively) are the smallest SWCNTs that could contain water molecules inside [14]. These diameters in SWCNTs are smaller than the corresponding diameters (6.95 Å and 8.59 Å) in SWSiCNTs. One may conclude that the entry of water molecules into SWSiCNTs is more difficult than that in SWCNTs because of the higher repulsion forces that silicon atoms in the SWSiCNTs have in comparison with the homogenous walls of pure SWCNTs. This repulsion may be due to the high polarizability (as seen in the values of the Lenard-Jones parameters) and the negative partial charge of silicon atoms. However, a clear decision about this subject needs a careful PMF analysis (see Section 3.5 for further discussion about the entrance of water molecules inside SWSiCNTs).

In wider SWSiCNTs, the arrangements of water molecules inside SWSiCNTs involve layered structures. The possible structures of water molecules inside SWSiCNTs will be discussed in the next section. Water molecules form one-layer cylinder-shaped tubes in the interior side of (6,6) and (12,0) SWSiCNTs with diameters of 10.31 Å and 11.90 Å, respectively (Fig. 5(e) and (f)). The formation of a layered structure is similar to what forms on the exterior side of nanotubes and, in the following, will be explained with respect to the potential energy variations. The variation of water structures from wire structures inside the (7,0), (8,0) and (5,5) SWSiCNTs to the solid-like cylinder-shaped tubes inside (6,6) and (12,0) SWSiCNTs could be the reason for the sudden decrease in diffusion coefficients that was observed in the previous section. In (8,8) and (14,0) SWSiCNTs with respective diameters of 13.75 Å and 13.89 Å, there are cylinders with wire structures of water molecules along the cylinder (Fig. 5(g) and (h)), and inside the (9,9) and (16,0) SWSiCNTs (with diameters of 15.47 Å and 15.88 Å, respectively, Fig. 5(i) and (j)), there are two concentric cylindrical structures of water molecules. Moreover, the second increase in the diffusion coefficient of confined water inside (6,6) and (12,0) SWSiCNTs compared with that inside (8,8) and (14,0) SWSiCNTs in Fig. 4 could be related to the appearance of a wire structure in the middle of the cylinder-like water structure in (6,6) and (12,0) SWSiCNTs that could diffuse faster. In the wider SWSiCNTs, such as (18,0) and (10,10) with respective diameters of 17.86 Å and 17.19 Å, water molecules are disordered (look at the snapshots that do not show any order structures in the regions near the center of nanotubes) are distributed in a bulk-like mode (see Fig. 5(k) and (l)). It can be seen in Fig. 5(k) that in the distances about 0–2 Å from the nanotube center the radial density of water molecules is going to be in close proximity to the value of bulk water outside the nanotube, in the distances about 16 Å and above. It seems that by increasing the nanotube diameter, the water molecules placed in the center of these wide nanotubes do not experience the presence of the walls and, therefore, they present the same structure as bulk water (and the diffusion coefficients are going to increase to reach bulk-like values). The bulk-like mode for water structures inside sufficiently wide nanotubes have been observed previously for SWCNTs [15]. These observations imply a basic characteristic of confined water inside the SWSiCNT: the dominant effect of the nanotube diameter on the structure of water molecules inside the SWSiCNT.

To investigate the helicity effect on the water molecule configurations inside SWSiCNTs, the water structures inside the SWSiCNTs in each row in Fig. 5 (with almost the same diameters) were compared. The comparisons demonstrated that there is no general dissimilarity between equilibrium configurations of water molecules in the interior of armchair and zigzag SWSiCNTs with the same diameters. These observations are in agreement with what has been previously reported for the effect of helicity on the entry of water molecules into SWCNTs [14,19]. An interesting exception to this general trend in Fig. 5 is that in spite of that fact that (7,0) and (4,4) nanotubes have almost the same diameters (6.947 Å and 6.875 Å, respectively), water molecules enter the (7,0) SWSiCNT, whereas they cannot enter the (4,4) SWSiCNT. This may be related to the fact that a water molecule entering an armchair tube would encounter a ring of positive and negative charges, whereas a water molecule approaching the entrance to a zigzag tube would encounter a ring of either positive or negative charges. These types of charge distributions make entering the water molecules impossible inside the narrow zigzag SWSiCNT, even if it has a diameter equal to the corresponding armchair nanotube. To further inspect the helicity effect on the water molecule configurations inside SWSiCNTs, the water configuration inside a group of SWSiCNTs with the same diameters (approximately 12 Å) and different helicities of (7,7), (12,0), (11,2), (9,5), and (8,6) are presented in Fig. 6. As shown, the water configurations are nearly the same in these nanotubes. Therefore, the examinations suggest that the helicity effect on the entrance of water molecules inside SWSiCNTs is influential just in narrow nanotubes. The PMF analysis also could be a good instrument for studying the helicity effect on the water molecule configurations inside SWSiCNTs. For more discussion about the energy barrier for entrance into armchair and zigzag SWSiCNTs, see Section 3.5 and Fig. 9.

As a whole, Figs. 5 and 6 show that the nanotube diameter plays important role in the structure of water molecules confined inside the SWSiCNT, but also show the slight effect of nanotube helicity on these structures.

Additionally, it would be useful to formulate the relationship between the nanotube diameters and the number of water layer structures inside SWSiCNTs. From the two basic characteristics of the distribution of water molecules inside the nanotube, it can be concluded that an SWSiCNT should have a diameter of D_n to have n layers of water molecules inside:

$$D_n = 2(\sigma_{SiO} + (n-1)\sigma_{OO}) \quad \text{for} \quad 1 \le n \le 5 \tag{6}$$

In this equation, σ_{OO} and σ_{SiO} are the Lennard–Jones repulsion parameters between oxygen–oxygen and silicon–oxygen atoms, respectively. This relation is similar to a relation previously established for SWCNTs [14], but the dominant repulsive atom here is the silicon atom. Using the above equation, an SWSiCNT is supposed to have diameters of 6.689 Å and 13.191 Å, which would contain

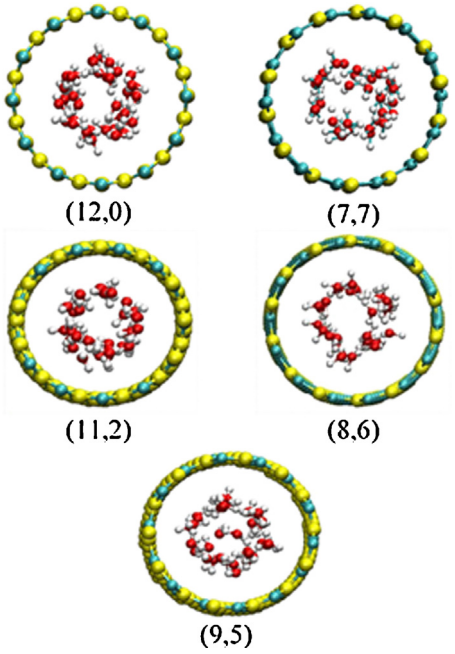

Fig. 6. The water configurations inside SWSiCNTs with the same diameters (approximately 12 Å) and different helicities. The color pattern of atoms is represented the same way as in Fig. 5. (For interpretation of the references to colour in this figure legend, the reader is referred to the web version of the article.)

one water layer (single-file) and two water layers (a cylinder shape water structure) inside, respectively. It should be noted that the diameter D_n is the diameter required to form a complete layer and that the SWSiCNTs with smaller diameters may enclose deficient layers of water molecules, as revealed in Fig. 5.

Furthermore, the distribution of water molecules outside the SWSiCNTs would be interesting because we can figure out that what happens for the arrangement of water molecules in a container of water when an SWSiCNT is immersed into it. If the blue line in every density profile in Fig. 5 considered as the nanotube wall, it is illustrated that there are two oxygen density peaks at approximately 3.4 Å from this blue line in the inner and outer side of the SWSiCNTs. This means that the water-nanotube interface has a thickness of approximately 7 Å. Therefore, for distances near the exterior side of the nanotube surface, the potential energy, caused by nonbonded interactions between the water molecules and the nanotube atoms, has the lowest value (at approximately 3.44 Å). The location of this first peak outside the nanotube could be logically interpreted by considering the repulsive part of the Lennard–Jones potential with $\sigma_{SiO} = 3.445$ Å . Going further from the first peak outside the nanotubes, the potential energy first increases and forms an energetically unfavorable region for the accommodation of water molecules (the distance between the two peaks outside the nanotube) and then (with increasing the distance more), another oxygen density peak appears at approximately 6.9 Å from the blue line in Fig. 5, referring to σ_{OO}. This second peak is caused by increasing the attraction part of the potential energy. Also, the location of this peak could also be related to the repulsive part of the Lennard–Jones potential with $\sigma_{OO} = 3.15061$ Å . Accordingly, water molecules constitute typical layered structures outside all SWSiCNTs, regardless of their diameters or helicities (unlike the interior density profiles). These attributes have been observed before in the analogous SWCNTs [58].

Another notable aspect of these density profiles, appears in comparison between empty spaces inside and outside of SWCNTs. From Fig. 5, it could be shown that (although this feature is not obvious in some cases especially wider ones in this figure) the empty spaces inside the nanotubes are somewhat larger than those outside. For example, in (14,0) SWSiCNTs, the void space between the inside face of the nanotube wall and the layered structure of water molecules is approximately 2.8 Å (the distance between the first oxygen peak inside the nanotube and the blue line), but the vacant space between the nanotube wall and the bulk water structure surrounding the nanotube is approximately 2.3 Å (the distance between the blue line and the fist peak outside the nanotube). This argument is more obvious in narrower SWSiCNTs, such as (8,0) SWSiCNTs, which have a void space of approximately 3 Å inside and 2.2 Å outside (the distances between the blue line and the fist oxygen peaks inside and outside the nanotube, respectively). These differences could be explained by considering that there are two forces that applied to water molecules inside the SWSiCNTs, the surface effects and the confinement effects (the applying forces from two opposite walls). However in the outside these nanotubes, there are a just surface effects from the outside face of the nanotube wall. The lack of nanoscale confinement effects in the exterior part of nanotubes makes the empty space smaller on this side. These results constitute the first report about the structural properties of water molecules surrounding SWSiCNTs.

3.4. Hydrogen bonding network of confined water molecules

The hydrogen bonding (HB) network among water molecules is the cause of the unique characteristics of water, especially in the solid and liquid phases, and many thermodynamic properties of water depend on the HB network. Namely, the HB network is the main factor in the phase transitions of water between different phases, such as between the liquid and the solid phase. For this reason, determination of the HB number and strength would be an exciting finding in the study of the phase transitions of water under confinement [60]. As another illustration, decreasing the number of HBs could result in increasing the diffusion rate of water molecules inside a nanotube, even if the confinement effect makes the water molecule movements slower than that in bulk water [40,61]. So, there are two opposite parameters for determination of the diffusion coefficients. First, HBs that increase the diffusion rate of water molecules inside a nanotube and second, the surface effect that decrease the water molecule movements inside the nanotubes. It is assumed that there is a nanotube diameter gauge in which the HB network is the dominant factor for determination of thermodynamic properties. Hence, it could be interesting to study the average number of HBs per water molecule inside the SWSiCNTs, $\langle n_{HB} \rangle$, in the search for gauge in which the HB network overcomes the confinement effect. HB in this work is defined as a weak chemical bond formed when a slightly positive hydrogen atom of one water molecule is attracted to the slightly negative oxygen atom of another water molecule. Here, the number of hydrogen bonds is defined as the number both donor and acceptors per water molecule (equals to four for a bulk water molecule). Geometrical conditions were considered to define a criterion for the existence of the hydrogen bond between two water molecules inside SWSiCNTs. First, the distance between the oxygen atoms of two water molecules has to be smaller than a threshold value of 3 Å. Second, the bond angle among the O—O path and the molecular O—H direction, where H is the acceptor atom in the hydrogen bond formation, is required to be less than a definite threshold value of 30°.

Keeping these conditions in mind, the variation of $\langle n_{HB} \rangle$ for armchair and zigzag SWSiCNTs vs. nanotube diameter are plotted in Fig. 7. The number of HBs per water molecule in bulk in this figure was obtained by performing a simulation of 3000 TIP3P water molecules with a density equal to the bulk density and under conditions similar to those in other systems simulated in this work. Fig. 7 shows that $\langle n_{HB} \rangle$ inside SWSiCNTs is always lower than

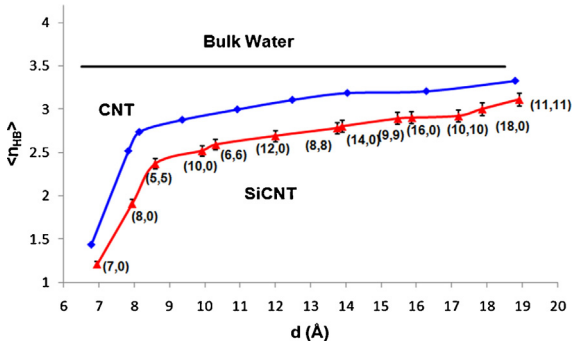

Fig. 7. Number of hydrogen bonds per water molecule, $\langle n_{HB} \rangle$, vs. the nanotube diameter, d.

that of bulk water. With the SWSiCNTs that are calculated in this figure, the red and black curves are not asymptotes, but it is predicted that by increasing the diameter (for example, in (16,16) SWSiCNTs), the red curve is going to be an asymptote of the bulk water curve (black link). In narrower nanotubes, the void space that was mentioned previously has more value with respect to the whole volume of the tube, but in larger nanotubes, because of the larger volume that these tubes have, the effect of the empty space is going to be less important. Water molecules would be able to form more HBs per molecule and would have more space to construct a HB network. Thus, confinement effects diminish the number of HBs in the water structure network. Moreover, it is found that in the narrowest nanotube, there is only approximately one HB per water molecule. This finding is in agreement with what is just reported in this paper about the wire structure of water molecules in narrow SWSiCNTs (see Figs. 7 and 5).

Another fascinating consideration in Fig. 7 is the sensitivity of $\langle n_{HB} \rangle$ value to the nanotube diameter in narrow and large SWSiCNTs. In narrow SWSiCNTs, $\langle n_{HB} \rangle$ is very sensitive to the nanotube diameter. For example, (5,5) SWSiCNT with a diameter of 8.59 Å has an $\langle n_{HB} \rangle$ value equal to 2.37, while an (8,0) SWSiCNT with a diameter of 7.939 Å has a much smaller $\langle n_{HB} \rangle$ value of approximately 1.91. However, in larger nanotubes such as (8,8) and (18,0) SWSiCNTs, (with diameters of 13.75 Å and 17.86 Å, respectively), the $\langle n_{HB} \rangle$ values are almost the same (2.78 and 3, respectively). The trends of $\langle n_{HB} \rangle$ sensitivity to the diameter are the same as those that have been found for SWCNTs [14]. As shown in Fig. 7, there is no significant difference between the $\langle n_{HB} \rangle$ in armchair and zigzag SWSiCNTs. Therefore, it can be concluded that the significant differences between the diffusive behavior of these two types of SWSiCNTs is not related to the number of hydrogen bonds between water molecules confined inside them.

Moreover, Fig. 7 shows that confinement lead to a significant loss of the number of hydrogen bonds among water molecules inside SWSiCNTs in comparison with what is presented inside SWCNTs, regardless of SWSiCNT helicities. This means that the water molecules inside SWSiCNTs are freer to move along the nanotube axis and could be in a different phase from water molecules inside an SWCNT with the same diameter. In addition, it could be predicted that inside the SWSiCNTs, the diffusion rate of water molecules is larger than that in SWCNTs (see Fig. 4).

The results also demonstrated that in narrow SWSiCNTs, there are two effects that could act oppositely, as was reported for the similar case of SWCNTs [14]. The surface effect on the water molecules causes a decrease in the movement of water molecules (this effect is not studied in this paper directly, but it exists in systems that consist a surface and interface area), while at the same time, confinement leads to a decrease in $\langle n_{HB} \rangle$ that makes the water molecules freer to move throughout the nanotube than in bulk water (with an $\langle n_{HB} \rangle$ of approximately 3.5). However, in

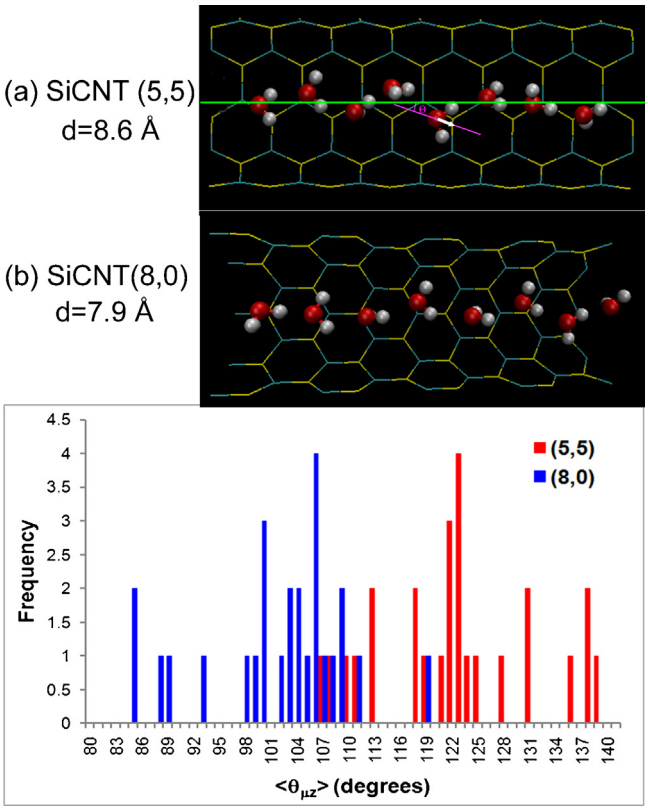

Fig. 8. (a) Side view of the wire structure of water molecules inside (5,5) and (8,0) SWSiCNTs. The angle $\theta_{\mu z}$ as the angle between the nanotube main axis along the z direction (the green line) and a water molecule dipole (the white arrow) is shown here. (b) The orientation of water molecule dipoles inside (5,5) and (8,0) SWSiCNTs as a function of simulation time for 5 ps of simulation. (For interpretation of the references to colour in this figure legend, the reader is referred to the web version of the article.)

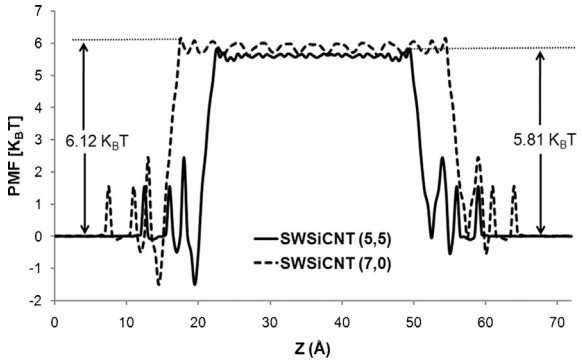

Fig. 9. PMF of water molecules along the nanotube axial direction for a (5,5) SWSiCNT (solid) and a (7,0) SWSiCNT (dashed). The (5,5) SWSiCNT is placed from 22.5 to 49.5 Å and the (7,0) SWSiCNT is located from 17.5 to 54.5 Å.

larger nanotubes, $\langle n_{HB} \rangle$ does not change significantly, and the surface effect would be the dominant effect. The surface effects will be discussed more in the next section.

3.5. Orientation of water molecule dipole moments

The orientation of water dipole moments is a comprehensible point for predicting the surface effect of nanotube walls. The orientation of water molecule dipoles, $\theta_{\mu z}$, could be described as the angle between the nanotube main axis along the z direction (the green line in Fig. 8(a)) and the water molecule dipole (the white arrow in Fig. 8(a)). If the water dipole vector is along the positive

direction of the z axis, $\theta_{\mu z}$ equals 0°, while for the water dipole vector perpendicular to the nanotube main axis, $\theta_{\mu z}$ equals 90°.

As noted in the previous sections, the (5,5) and (8,0) SWSiCNTs could be appropriate for the surface effect study because they are the narrowest SWSiCNTs that permit water molecules to enter, and the water molecules have a one-dimensional wire structure inside. The water structure and the average of the orientation of water molecule dipoles $\langle\theta_{\mu z}\rangle$ inside (5,5) and (8,0) SWSiCNTs in each time step for over 5 ps of the whole simulation time of 3 ns is shown in Fig. 8. As illustrated, there are small fluctuations in the $\langle\theta_{\mu z}\rangle$ values and favorable arrangement of the confined water wire along the nanotube axis. In addition, our results show that (it is not shown in Fig. 8) when a water molecule in the wire structure flips, other water molecules reverse their orientations concurrently; hence, the total orientation of all water molecules inside the nanotube does not change. The basis of this event involves the strong electrostatic interactions and strong HB network among water molecules in the wire structure.

Furthermore, Fig. 8 indicates that in the (5,5) SWSiCNT, where the nanotube diameter is larger than that of (8,0) SWSiCNTs (8.594 Å and 7.939 Å, respectively), $\langle\theta_{\mu z}\rangle$ has unexpectedly larger values than in (8,0) SWSiCNTs. This is an unpredicted result because the larger (5,5) SWSiCNTs have more space for the water molecule to flip, and so the mean value of $\langle\theta_{\mu z}\rangle$ should be smaller than that in (8,0) SWSiCNTs. This irregular water molecule orientation may be related to the differences between the magnitude and direction of the electrostatic field induced by C and Si atom arrangements on the walls if armchair and zigzag SWSiCNTs. So, this result could be assumed as an evidence of correlation between nanotube helicity and water molecule structures inside SWSiCNTs. Although some more clear evidences are needed to be sure about this assumption, but this observation could be an interesting beginning for beginning for performing a thorough investigation on this correlation. If this correlation comes true, it could cleanly explain the faster axial diffusion of water molecules inside armchair SWSiCNTs because the bigger $\langle\theta_{\mu z}\rangle$ values mean that the water molecules do not rotate frequently and so could pass through the tube faster that is possible in zigzag SWSiCNTs. This is the first time that the nanotube helicity has been directly correlated to water molecule structures inside SWSiCNTs, and this provides motivation for a comprehensive study of the helicity effect on confined water structures.

A comparison between the results in Fig. 8 and water dipole orientations inside SWCNTs would be interesting. Mann et al. [62] reported that the $\langle\theta_{\mu z}\rangle$ value for water molecules inside a (6,6) SWCNT changes in a range of 120–135° for a period of 5 ps. The $\langle\theta_{\mu z}\rangle$ for water molecules inside SWSiCNTs have lower values regardless of the nanotube helicity. This difference may be related to the significant difference in partial charges on the wall atoms in SWSiCNTs in comparison with the homogenous wall in the SWCNT. In another investigation, Won et al. [20] showed that water molecules inside (10,0) SWCNTs have an orientation more normal to the nanotube axis than that inside (6,6) SWCNTs. The trend of these results is in good agreement with what is reported here for SWSiCNTs. Accordingly, wire water structures inside SWSiCNTs could be a better water diffusive medium than those inside SWCNTs due to the more vertical arrangement they have there.

The different entrance of a water molecule into the (5,5) and (7,0) SWSiCNT could be clarified by the potential of mean force (PMF) analysis [63]. The mean force distribution, associated with entrance of a water molecule into the nanotube, was calculated by sampling the force feels by the water molecules in a bin. As shown in Fig. 9, the energy barrier is 5.81 K_BT for (5,5) SWSiCNT and 6.12 K_BT for (7,0) SWSiCNT. This amount of barrier energy is approximately acceptable because it has been shown that an energy barrier of about 5 K_BT is small for permeation of water molecules [64]. Also, the energy barriers for other types of nanotubes were reported to be 5.29 K_BT for the (5,5) SWBNNT, 9.83 K_BT for the (5,5) SWCNT [65] and 9.83 K_BT for (6,6) SWCNT [20]. So, SWSiCNTs are less favorable for the water molecule to enter inside the nanotube compared to SWCNTs and SWBNNTs (see Section 3.3). In addition, as illustrated in Fig. 9, the more probability for the water to overcome the energy barrier in armchair SWSiCNTs could be explained the relative ease with which a water molecule can enter armchair vs. zigzag nanotubes. Furthermore, Fig. 9 shows more fluctuations in PMF values inside (7,0) SWSiCNT compared to (5,5) SWSiCNT. This future could be a justification for faster diffusion of water molecules inside armchair SWSiCNT vs. zigzag ones.

4. Conclusions

We have performed a series of MD simulations of water molecules confined in SWSiCNTs, either zigzag or armchair with different diameters, to investigate the nanotube diameter and helicity effects on the static and dynamic properties of confined water molecules. In this work, the first outcomes of molecular dynamics simulations presenting the overall density of confined water molecules inside SWSiCNTs are reported, and a satisfying correlation between the overall density and the nanotube diameters is proposed. Additionally, a correction factor for this equation for narrower SWSiCNTs, which have a different overall density variation vs. nanotube diameter, is applied.

The transport properties of water confined in armchair and zigzag SWSiCNTs of various diameters is investigated, for the first time, using molecular dynamics simulation. The mean square displacement (MSD) of water molecules confined inside all SWSiCNTs follows a ballistic-type mechanism on production times less than several hundreds of picoseconds. However, when the MSDs are analyzed beyond 1 ns, the simulation results show that the diffusion mechanism changes and becomes single-file in narrow SWSiCNTs (with diameters less than 10 Å), while in wider SWSiCNTs, the diffusion mechanism changes to Fickian. These results show that the diffusion mechanism of water molecules inside narrow SWSiCNTs is different from what has been reported for SWCNTs and SWBNNTs in previous studies. It is also demonstrated that the wetting behavior of water molecules confined inside SWSiCNTs is better than that of SWCNTs and SWBNNTs with a similar diameter.

Radial density profiles reveal that SiCNTs could be filled up by water molecules in three different ways—including single-file wire, layered, and bulk structures—depending on the nanotube diameter, while nanotube helicity exerts little effect on the structural properties of water. By taking the slight helicity effect and remarkable nanotube diameter effect on the confined water structure into account, an equation is suggested for prediction of the nanotube required diameter to form n structural layers inside SWSiCNTs. In contrast, it is revealed that the distribution of water molecules outside nanotubes, where there are no confinement effects, is the same for all different nanotube diameters and helicities. The unusual diffusive behavior of water molecules confined inside SWSiCNTs could be interpreted by considering these three different types of filling behaviors.

The average number of HBs per water molecule $\langle n_{HB}\rangle$, an essential characteristic in determination of the state and thermodynamic properties of confined water, was calculated. The results showed that the confinement effects reduce the number of HBs in the water structure network in comparison with that in bulk water. Furthermore, $\langle n_{HB}\rangle$ for water molecules within SWSiCNTs is always lower than that in SWCNTs, regardless of SWSiCNTs helicities. Thus, confined water inside SWSiCNTs could be in a state different from that in SWCNTs with the same diameter. In addition, the $\langle n_{HB}\rangle$ value is much more sensitive to the nanotube diameter in narrower SWSiCNTs due to the large confinement effects of nanotube

walls. Generally, the surface and confinement effects are competing to determine the average number of HBs per water molecule. In narrower SiCNTs, the confinement effect controls the $\langle n_{HB} \rangle$ values, while in larger nanotubes, the surface effect is dominant.

Finally, the orientation of confined water molecule dipoles inside narrow SWSiCNTs was investigated for the first time to investigate the probable use of encapsulated wire water structures as a proton conductive medium. The difference between the orientation of the single-file water structure inside zigzag (with diameters larger than the other nanotubes) and armchair SWSiCNTs proved that the nanotube helicity determines the orientations of the water molecules inside. This result and also the results of PMF analysis make clear the noticeable difference between the diffusion coefficients of water confined inside armchair and zigzag SWSiCNTs. Consequently, wire water structures inside SWSiCNTs could be a better water diffusive medium than that inside SWCNTs due to the more vertical arrangement they have there. It should be noted that the water molecules are considered to be fixed here. In smaller diameter tubes, buckling of the structure occurs, which may affect the results.

To conclude, the MD investigation of systems including SWSiCNTs with encapsulated water molecules inside encourages application of SWSiCNTs as artificial water channels in nanoscale biological or electrical environments.

Appendix A. Supplementary data

Supplementary data associated with this article can be found, in the online version, at http://dx.doi.org/10.1016/j.jmgm.2013.04.012.

References

[1] Y. Gogotsi, J.A. Libera, A. Guvenc-Yazicioglu, C.M. Megaridis, In situ multiphase fluid experiments in hydrothermal carbon nanotubes, Applied Physics Letters 79 (2001) 1021–1023.

[2] K. Murata, K. Mitsuoka, T. Hirai, T. Walz, P. Agre, J.B. Heymann, A. Engel, Y. Fujiyoshi, Structural determinants of water permeation through aquaporin-1, Nature 407 (2000) 599–605.

[3] M. Weik, U. Lehnert, G. Zaccai, Liquid-like water confined in stacks of biological membranes at 200 K and its relation to protein dynamics, Biophysical Journal 89 (2005) 3639–3646.

[4] V. Sazonova, Y. Yaish, H. Ustunel, D. Roundy, T.A. Arias, P.L. McEuen, A tunable carbon nanotube electromechanical oscillator, Nature 431 (2004) 284–287.

[5] J.K. Holt, H.G. Park, Y. Wang, M. Stadermann, A.B. Artyukhin, C.P. Grigoropoulos, A. Noy, O. Bakajin, Fast mass transport through sub-2-nanometer carbon nanotubes, Science 312 (2006) 1034–1037.

[6] T. Nanok, N. Artrith, P. Pantu, P.A. Bopp, J. Limtrakul, Structure and dynamics of water confined in single-wall nanotubes, Journal of Physical Chemistry A 113 (2008) 2103–2108.

[7] W. Wenseleers, S. Cambré, J. Čulin, A. Bouwen, E. Goovaerts, Effect of water filling on the electronic and vibrational resonances of carbon nanotubes: characterizing tube opening by Raman spectroscopy, Advanced Materials 19 (2007) 2274–2278.

[8] H. Kyakuno, K. Matsuda, H. Yahiro, Y. Inami, T. Fukuoka, Y. Miyata, K. Yanagi, Y. Maniwa, H. Kataura, T. Saito, M. Yumura, S. Iijima, Confined water inside single-walled carbon nanotubes: global phase diagram and effect of finite length, Journal of Chemical Physics 134 (2011) 244501–244514.

[9] S. Cambré, B. Schoeters, S. Luyckx, E. Goovaerts, W. Wenseleers, Experimental observation of single-file water filling of thin single-wall carbon nanotubes down to chiral index (5,3), Physical Review Letters 104 (2010) 207401.

[10] Y.J. Wang, L.Y. Wang, Water chain encapsulated in carbon nanotube revealed by density functional theory, International Journal of Quantum Chemistry 111 (2011) 4465–4471.

[11] A. Alexiadis, S. Kassinos, Molecular simulation of water in carbon nanotubes, Chemical Reviews 108 (2008) 5014–5034.

[12] S. Javadian, F. Taghavi, F. Yari, S.M. Hashemianzadeh, Phase transition study of confined water molecules inside carbon nanotubes: hierarchical multiscale method from molecular dynamics simulation to ab initio calculation, Journal of Molecular Graphics and Modelling 38 (2012) 40–49.

[13] A. Striolo, The mechanism of water diffusion in narrow carbon nanotubes, Nano Letters 6 (2006) 633–639.

[14] J. Wang, Y. Zhu, J. Zhou, X.H. Lu, Diameter and helicity effects on static properties of water molecules confined in carbon nanotubes, Physical Chemistry Chemical Physics 6 (2004) 829–835.

[15] A. Alexiadis, S. Kassinos, The density of water in carbon nanotubes, Chemical Engineering Science 63 (2008) 2047–2056.

[16] J. Marti, M.C. Gordillo, Time-dependent properties of liquid water isotopes adsorbed in carbon nanotubes, Journal of Chemical Physics 114 (2001) 10486–10492.

[17] J. Marañón Di Leo, J. Marañón, Confined water in nanotube, Journal of Molecular Structure: THEOCHEM 623 (2003) 159–166.

[18] T.W. Allen, S. Kuyucak, S.H. Chung, The effect of hydrophobic and hydrophilic channel walls on the structure and diffusion of water and ions, Journal of Chemical Physics 111 (1999) 7985–7999.

[19] R.J. Mashl, S. Joseph, N.R. Aluru, E. Jakobsson, Anomalously immobilized water: a new water phase induced by confinement in nanotubes, Nano Letters 3 (2003) 589–592.

[20] C.Y. Won, S. Joseph, N.R. Aluru, Effect of quantum partial charges on the structure and dynamics of water in single-walled carbon nanotubes, Journal of Chemical Physics 125 (2006) 114701–114709.

[21] A. Berezhkovskii, G. Hummer, Single-file transport of water molecules through a carbon canotube, Physical Review Letters 89 (2002) 064503.

[22] H. Fang, R. Wan, X. Gong, H. Lu, S. Li, Dynamics of single-file water chains inside nanoscale channels: physics, biological significance and applications, Journal of Physics D: Applied Physics 41 (2008) 103002.

[23] C.W. Lam, J. James, R. McCluskey, S. Arepalli, R. Hunter, A review of carbon nanotube toxicity and assessment of potential occupational and environmental health risks, Critical Reviews in Toxicology 36 (2006) 189–217.

[24] L.Z. Pei, Y.H. Tang, Y.W. Chen, C. Guo, X.X. Li, Y. Yuan, Y. Zhang, Preparation of silicon carbide nanotubes by hydrothermal method, Journal of Applied Physics 99 (2006), 114306-114306.

[25] A. Huczko, M. Bystrzejewski, H. Lange, A. Fabianowska, S. Cudziło, A. Panas, M. Szala, Combustion synthesis as a novel method for production of 1-D SiC nanostructures, Journal of Physical Chemistry B 109 (2005) 16244–16251.

[26] T. Taguchi, N. Igawa, H. Yamamoto, S. Jitsukawa, Synthesis of silicon carbide nanotubes, Journal of the American Ceramic Society 88 (2005) 459–461.

[27] C. Zhi, Y. Bando, C. Tang, D. Golberg, Boron nitride nanotubes, Materials Science and Engineering: R: Reports 70 (2010) 92–111.

[28] T.A. Hilder, D. Gordon, S.-H. Chung, Salt rejection and water transport through boron nitride nanotubes, Small 5 (2009) 2183–2190.

[29] C.Y. Won, N.R. Aluru, Structure and dynamics of water confined in a boron nitride nanotube, Journal of Physical Chemistry C 112 (2008) 1812–1818.

[30] K. Adhikari, A.K. Ray, Carbon- and silicon-capped silicon carbide nanotubes: an ab initio study, Physics Letters A 375 (2011) 1817–1823.

[31] H.L. Chen, S.P. Ju, J.S. Lin, J. Zhao, H.T. Chen, J.G. Chang, M. Weng, S.C. Lee, W.J. Lee, Electronic properties of a silicon carbide nanotube under uniaxial tensile strain: a density function theory study, Journal of Nanoparticle Research 12 (2010) 2919–2928.

[32] S. Jiuxu, Y. Yintang, L. Hongxia, G. Lixin, Z. Zhiyong, Electronic transport properties of the armchair silicon carbide nanotube, Journal of Semiconductors 31 (2010) 114003.

[33] M. Menon, E. Richter, A. Mavrandonakis, G. Froudakis, A.N. Andriotis, Structure and stability of SiC nanotubes, Physical Review B 69 (2004), 115322-115321-115322-115324.

[34] Y. Zhang, H. Huang, Stability of single-wall silicon carbide nanotubes – molecular dynamics simulations, Computation Materials Science 43 (2008) 664–669.

[35] A. Mavrandonakis, G.E. Froudakis, M. Schnell, M. Mühlhäuser, From pure carbon to silicon–carbon nanotubes: an ab-initio study, Nano Letters 3 (2003) 1481–1484.

[36] K.M. Alam, A.K. Ray, A hybrid density functional study of zigzag SiC nanotubes, Nanotechnology 18 (2007) 495706.

[37] K.M. Alam, A.K. Ray, Hybrid density functional study of armchair SiC nanotubes, Physical Review B: Condensed Matter 77 (2008) 035436.

[38] M. Zhao, Y. Xia, F. Li, R.Q. Zhang, S.T. Lee, Strain energy and electronic structures of silicon carbide nanotubes: density functional calculations, Physical Review B 71 (2005) 085312.

[39] G. Mpourmpakis, G.E. Froudakis, G.P. Lithoxoos, J. Samios, SiC nanotubes: a novel material for hydrogen storage, Nano Letters 6 (2006) 1581–1583.

[40] M. Khademi, M. Sahimi, Molecular dynamics simulation of pressure-driven water flow in silicon-carbide nanotubes, Journal of Chemical Physics 135 (2011) 204507–204509.

[41] R. Yang, T.A. Hilder, S.H. Chung, A. Rendell, First-principles study of water confined in single-walled silicon carbide nanotubes, Journal of Physical Chemistry C 115 (2011) 17255–17264.

[42] T.A. Hilder, R. Yang, D. Gordon, A.P. Rendell, S.-H. Chung, Silicon carbide nanotube as a chloride-selective channel, Journal of Physical Chemistry C 116 (2012) 4465–4470.

[43] H.J.C. Berendsen, J.P.M. Postma, W.F. van Gunsteren, A. DiNola, J.R. Haak, Molecular dynamics with coupling to an external bath, Journal of Chemical Physics 81 (1984) 3684–3690.

[44] The DL_POLY Classic User Manual, Daresbury Laboratory, United Kingdom, 2010.

[45] W.L. Jorgensen, J. Chandrasekhar, J.D. Madura, R.W. Impey, M.L. Klein, Comparison of simple potential functions for simulating liquid water, Journal of Chemical Physics 79 (1983) 926–935.

[46] K. Malek, M. Sahimi, Molecular dynamics simulations of adsorption and diffusion of gases in silicon-carbide nanotubes, Journal of Chemical Physics 132 (2010), 014310-014310.

[47] D. Tildesley, M. Allen, Computer Simulation of Liquids, Clarendon University Press, United Kingdom, 1987.

[48] J.H. Walther, R. Jaffe, T. Halicioglu, P. Koumoutsakos, Carbon nanotubes in water: structural characteristics and energetics, Journal of Physical Chemistry B 105 (2001) 9980–9987.
[49] A. Alexiadis, S. Kassinos, Self-diffusivity, hydrogen bonding and density of different water models in carbon nanotubes, Molecular Simulation 34 (2008) 671–678.
[50] G. Hummer, J.C. Rasaiah, J.P. Noworyta, Water conduction through the hydrophobic channel of a carbon nanotube, Nature 414 (2001) 188–190.
[51] B. Hosticka, P.M. Norris, J.S. Brenizer, C.E. Daitch, Gas flow through aerogels, Journal of Non-Crystalline Solids 225 (1998) 293–297.
[52] J. Martí, M.C. Gordillo, Temperature effects on the static and dynamic properties of liquid water inside nanotubes, Physical Review E 64 (2001) 021504.
[53] D.G. Levitt, Dynamics of a single-file pore: non-Fickian behavior, Physical Review A 8 (1973) 3050–3054.
[54] Y.-C. Liu, J.-W. Shen, K.E. Gubbins, J.D. Moore, T. Wu, Q. Wang, Diffusion dynamics of water controlled by topology of potential energy surface inside carbon nanotubes, Physical Review B 77 (2008) 125438.
[55] Y. Liu, Q. Wang, Transport behavior of water confined in carbon nanotubes, Physical Review B 72 (2005) 085420.
[56] K. Koga, G.T. Gao, H. Tanaka, X.C. Zeng, Formation of ordered ice nanotubes inside carbon nanotubes, Nature 412 (2001) 802–805.
[57] T. Kurita, S. Okada, A. Oshiyama, Energetics of ice nanotubes and their encapsulation in carbon nanotubes from density-functional theory, Physical Review B 75 (2007) 205424.
[58] L.L. Huang, Q. Shao, L.H. Lu, X.H. Lu, L.Z. Zhang, J. Wang, S.Y. Jiang, Helicity and temperature effects on static properties of water molecules confined in modified carbon nanotubes, Physical Chemistry Chemical Physics 8 (2006) 3836–3844.
[59] Y. Zhu, M. Wei, Q. Shao, L. Lu, X. Lu, W. Shen, Molecular dynamics study of pore inner wall modification effect in structure of water molecules confined in single-walled carbon nanotubes, Journal of Physical Chemistry C 113 (2008) 882–889.
[60] S. Javadian, F. Taghavi, F. Yari, S.M. Hashemianzadeh, Phase transition study of confined water molecules inside carbon nanotubes: hierarchical multiscale method from molecular dynamics simulation to Ab Initio calculation, Journal of Molecular Graphics and Modelling (2012), http://dx.doi.org/10.1016/j.jmgm.2012.1005.1009.
[61] J.A. Thomas, A.J.H. McGaughey, O. Kuter-Arnebeck, Pressure-driven water flow through carbon nanotubes: Insights from molecular dynamics simulation, International Journal of Thermal Sciences 49 (2010) 281–289.
[62] D.J. Mann, M.D. Halls, Water alignment and proton conduction inside carbon nanotubes, Physical Review Letters 90 (2003) 195503.
[63] R. Kjellander, H. Greberg, Mechanisms behind concentration profiles illustrated by charge and concentration distributions around ions in double layers, Journal of Electroanalytical Chemistry 450 (1998) 233–251.
[64] B.L. de Groot, H. Grubmüller, The dynamics and energetics of water permeation and proton exclusion in aquaporins, Current Opinion in Structural Biology 15 (2005) 176–183.
[65] C.Y. Won, N.R. Aluru, Water permeation through a subnanometer boron nitride nanotube, Journal of the American Chemical Society 129 (2007) 2748–2749.